

TECHNICAL COMMUNICATION

# Reduction of Germanium Dioxide with Methane

M.C. ALTAY<sup>1,2</sup> and S. EROGLU<sup>1</sup>

1.—Department of Metallurgical and Materials Engineering, Engineering Faculty, Istanbul University - Cerrahpasa, 34320 Avcilar, Istanbul, Turkey. 2.—e-mail: mcumbul@istanbul.edu.tr

The reaction behavior of GeO<sub>2</sub> powder in CH<sub>4</sub> flow was investigated at 885–1075 K. Equilibrium thermodynamic analyses revealed that GeO<sub>2</sub> was reduced to Ge by CH<sub>4</sub>. Mass measurement, x-ray diffraction and scanning electron microscopy techniques were used to characterize the products. The reactivity between GeO<sub>2</sub> and CH<sub>4</sub> increased with the reaction temperature. The CH<sub>4</sub> decomposition at 1075 K sufficed for the reduction of GeO<sub>2</sub>. Substantial mass loss was observed at 1075 K which was attributed to the oxide sublimation in the form of GeO. The residue contained only GeO<sub>2</sub>. A powdery Ge deposit was obtained from the sublimated oxide in the downstream side of the reaction tube. It was proposed that the oxide sublimation and Ge formation took place by the reactions between the oxides and the by-products of CH<sub>4</sub> decomposition. This study may be extended to GeO<sub>2</sub>-containing scraps to produce Ge from them in CH<sub>4</sub> flow.

## INTRODUCTION

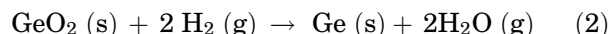
Ge is a relatively rare element, brittle, transparent in the infrared spectrum and a semiconductor. It has been increasingly used for numerous applications such as infrared night vision systems, jewels (Ag-Ge alloys), and stainless steel production. Ge is not found in the elemental state, it is extracted from various raw materials including ore concentrates, by-products of Zn extraction process and fly ash at coal-burning power plants. It is usually produced from GeO<sub>2</sub>, which is an intermediate product obtained by the processing of raw materials. Ge can be recovered from GeO<sub>2</sub>-containing scraps such as those of wide-angle camera lenses, optical fibers, and catalysts.<sup>1</sup>

GeO<sub>2</sub> is commonly reduced to the metal by H<sub>2</sub> and solid C. The C reduction of GeO<sub>2</sub> takes place via the following carbothermal reaction:



This reaction requires high temperatures (> 1473 K) and prolonged times owing to sluggish reaction kinetics between the solid reactants.<sup>2</sup> Furthermore, high-purity carbon is required to minimize contamination in Ge for electronic applications. Gas–solid reactions may reduce temperature and time owing to the direct contact between the reactants. For example, the H<sub>2</sub>

reduction of GeO<sub>2</sub> typically takes place at low temperatures, for instance at 800 K,<sup>3</sup> via the overall reaction:



The reduced product is purified by zone refinement techniques for use in electronic devices.<sup>1</sup>

CH<sub>4</sub>, a main component of natural gas, may be considered as an alternative reducing agent for GeO<sub>2</sub> because it is relatively cheap and contains H<sub>2</sub>. CH<sub>4</sub> has been used to reduce metal oxides such as Fe<sub>2</sub>O<sub>3</sub>,<sup>4</sup> NiO.<sup>5</sup> Little is known about the reaction of CH<sub>4</sub> with GeO<sub>2</sub>. Here, attempts were made to shed light on the following issues: (1) is the reduction of GeO<sub>2</sub> possible in a stream of CH<sub>4</sub>; (2) what are the optimal parameters (the temperature and time) to obtain Ge without free C; and (3) what is the reaction pathway leading to Ge from GeO<sub>2</sub> in CH<sub>4</sub> flow? Furthermore, understanding these issues may have practical implications for producing single-phase Ge from GeO<sub>2</sub>-containing scraps under CH<sub>4</sub> atmosphere. Accordingly, this study was undertaken to investigate the CH<sub>4</sub> reduction of GeO<sub>2</sub>.

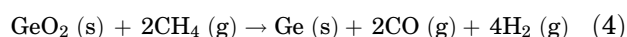
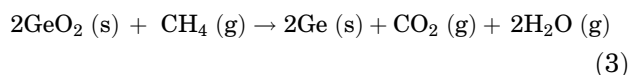
## THERMODYNAMIC CONSIDERATIONS

Prior to the experimental runs, a chemical equilibrium analysis of the Ge-O-C-H system was carried out to explore the possibility of the reduction of GeO<sub>2</sub> by CH<sub>4</sub>, and to assist in understanding the

process chemistry. The computational approach was based on Gibbs' free energy minimization method,<sup>6</sup> which does not require knowledge of specific reactions involved in a system. The equilibrium calculation gives a combination of the species, which satisfy the material balance and minimum free energy requirements at constant temperature and input reactant composition.

All possible species that may be present in a system and their thermodynamic data are needed at the temperatures studied. CO, CO<sub>2</sub>, CH<sub>4</sub>, H<sub>2</sub>, H<sub>2</sub>CO, C<sub>2</sub>H<sub>4</sub>, H<sub>2</sub>O, GeH<sub>4</sub>, GeO, and Ge were among the 62 gaseous species considered for the Ge-O-C-H system. Solid equilibrium phases were assumed to be pure GeO<sub>2</sub>, Ge, and C. Gibbs' free energy of formations of the constituents were obtained from the thermochemical tables.<sup>7,8</sup> Equilibrium compositions of gas and solid phases were computed as a function of temperature (1000–1300 K), and input CH<sub>4</sub> mole fraction ( $X_{\text{CH}_4} \approx 0-1$ ) at 1 atm using SOLGAS MIX software.  $X_{\text{CH}_4}$  is defined as  $n_{\text{CH}_4}^{\circ} / (n_{\text{CH}_4}^{\circ} + n_{\text{GeO}_2}^{\circ})$ , where  $n^{\circ}$  is the initial mole of the reactants.

Figure 1a shows the domains for the formation of the solid phases predicted as a function of temperature and  $X_{\text{CH}_4}$ . It can be seen that the GeO<sub>2</sub> + Ge, Ge, and Ge + C phase fields appear successively as  $X_{\text{CH}_4}$  increases from near zero to near unity. Single-phase Ge forms at intermediate CH<sub>4</sub> mole fractions, and its formation range increases with increasing temperature (for example, from 0.42–0.65 at 1100 K to 0.27–0.66 at 1300 K). At  $X_{\text{CH}_4}$  values higher than the upper limits, free C forms along with Ge. Figure 1b shows variation of the partial pressures of the gaseous species with  $X_{\text{CH}_4}$  at 1100 K. The relevant knowledge deduced from the figure may be summarized as follows. The main constituents of the gas phase are predicted to be CO<sub>2</sub>, CO, H<sub>2</sub>, H<sub>2</sub>O, CH<sub>4</sub>, and GeO. Minor species such as H<sub>2</sub>CO, C<sub>2</sub>H<sub>4</sub>, and GeH<sub>4</sub> with partial pressures less than 10<sup>-6</sup> atm are also present in the system. The partial pressures of H<sub>2</sub>O and CO<sub>2</sub> are higher than those of H<sub>2</sub> and CO, respectively, in the GeO<sub>2</sub> + Ge phase field ( $X_{\text{CH}_4} < 0.4$ ). In the Ge phase field ( $X_{\text{CH}_4} = 0.42-0.65$ ), H<sub>2</sub>, CO and CH<sub>4</sub> partial pressures increase while those of H<sub>2</sub>O and CO<sub>2</sub> decrease with increasing  $X_{\text{CH}_4}$ . Similar trends were determined at the other temperatures studied (for instance, at 1300 K; refer to online supplementary material Fig. S-1). It is also noticed from the figures that a significant amount of GeO species forms in the gas phase. The equilibrium analysis suggests that it is possible to reduce GeO<sub>2</sub> to Ge by CH<sub>4</sub>. The overall reduction reactions may be expressed as



## EXPERIMENTAL PROCEDURES

The experimental runs were carried out in a horizontal furnace equipped with a quartz tube (500 mm in length, 20 mm in diameter), SiC heating elements, and gas flow meters. Crystalline white GeO<sub>2</sub> powder (99.998%) supplied by Aldrich was used as delivered. Thermogravimetric analysis in Ar revealed that the oxide exhibited a slight mass loss (2.1 wt.%) owing to the moisture removal (refer to online supplementary material Fig. S-2).

The oxide powder (~ 0.05 g) in an alumina boat was inserted into the hot zone (~ 80 mm in length) of the quartz tube and heated to the reaction temperatures (885–1075 K) at a ramp rate of 15 K/min in Ar (99.999%). When the desired temperature was reached, undiluted CH<sub>4</sub> was allowed to flow (13.4 standard cubic centimeter per min, sccm) through the tube for various isothermal reaction times. After the reaction, Ar was flowed (42.5 sccm) again during cooling to room temperature. Mass measurements before and after the runs were carried out at room temperature by using a calibrated electronic balance with a sensitivity of ± 0.1 mg (Sartorius BP110S) to follow the extent of the reaction between the reactants. X-ray diffraction (XRD) analysis was carried in the 2θ range of 15°–90° using a diffractometer (Rigaku D/Max 2200) with a Cu radiation tube ( $\lambda_{\text{K}\alpha} = 0.154056$  nm). A scanning electron microscopy (SEM; FEI Quanta FEG 250) with an energy dispersive x-ray spectrometer (EDX) was used for the morphology studies.

## RESULTS AND DISCUSSION

### Effects of Temperature and Time

The oxide mass at 885 K essentially did not change within 60 min, indicating that the reaction of CH<sub>4</sub> with the oxide was negligible owing to the high CH<sub>4</sub> stability. The reactivity, however, increased with temperature, as revealed by Fig. 2, displaying the variations of the sample mass with the reaction times at 1025 K and 1075 K in CH<sub>4</sub> flow. The horizontal dashed line at 69.4 wt.% represents the theoretical mass for the complete conversion of GeO<sub>2</sub> to Ge. At 1025 K, the mass decreases to 63 wt.%, which is below the theoretical line as the reaction time is increased to 120 min. At 1075 K, the mass loss occurs at a faster rate. The mass is close to the theoretical value for the full reduction within 30 min. After 120 min reaction, it is 7.6 wt.% of the starting mass. It was noted that the mass loss was not accompanied by a change in color; the color of the residues was white.

Figure 3a shows the morphology of the GeO<sub>2</sub> powder as delivered. It consists of agglomerates with a size ranging from 5 μm to 22 μm. The higher magnification image (Fig. 3b) reveals that the agglomerates contain fine grains with a size of

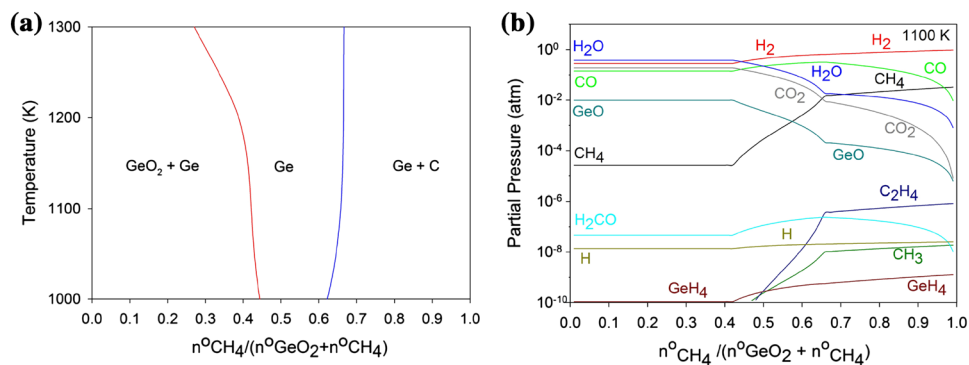


Fig. 1. (a) Equilibrium diagram showing the solid phases predicted as a function of temperature and  $X_{\text{CH}_4}$ . (b) Variation of partial pressure of the species with  $X_{\text{CH}_4}$  in equilibrium with the solid phases at 1100 K.

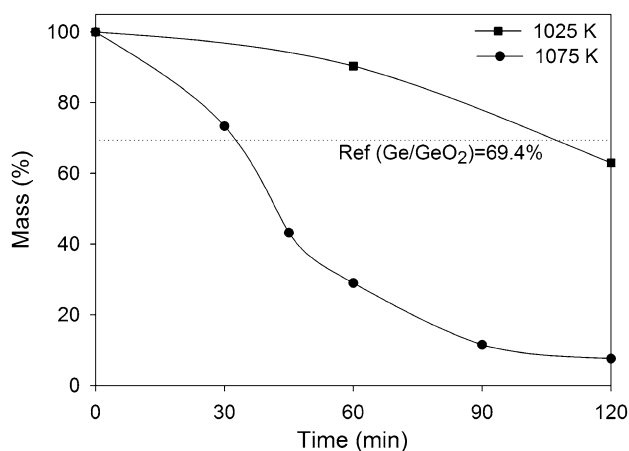


Fig. 2. Variation of the oxide mass ( $\text{GeO}_2$ ) with reaction time in  $\text{CH}_4$  flow at 1025 K and 1075 K.

0.1–0.4  $\mu\text{m}$ . After the reaction of the oxide with  $\text{CH}_4$  at 1075 K for 120 min, the morphology of the residue shows porous and whiskery features with etch pits (Fig. 3c). EDX analysis reveals O  $K_{\alpha}$ , Ge  $L_{\alpha,\beta}$ , Ge  $K_{\alpha}$ , and Ge  $K_{\beta}$  x-ray peaks at the energy levels of 0.50 keV, 1.20 keV, 9.85 keV, and 10.90 keV, respectively, suggesting that the residue in the boat is  $\text{GeO}_2$ .

### The Powdery Deposit by Downstream Side

It was noticed that the experimental runs at 1075 K resulted in a powdery black product deposited on the internal surface of the reaction tube by the downstream side. To facilitate morphology and phase analysis, the product was also allowed to deposit on a flat silicon  $\langle 100 \rangle$  substrate placed arbitrarily at 1050 K by the downstream side. Figure 4a shows the product formed on the Si substrate during the reaction between the  $\text{GeO}_2$  powder and  $\text{CH}_4$  for 120 min. As seen from the SEM image at low magnification, the deposit consists of fine particles and large platelets. The EDX analysis on this product (Fig. 4b) reveals Ge  $L_{\alpha,\beta}$ , Ge  $K_{\alpha}$ , and

Si  $K_{\alpha,\beta}$  x-ray peaks, but no peaks from oxygen and carbon are seen, suggesting that the deposit is metallic Ge. Furthermore, multifaceted grains with a size of the order of 1  $\mu\text{m}$  are observed as revealed by the side view of the deposit at a higher magnification (Fig. 4c). Rarely, whiskers with round particles at their tips or roots are also seen (Fig. 4d). EDX analysis (not shown) indicated that the whiskers contain only Ge.

### XRD Phase Analyses of the Residue and the Deposit

Figure 5a and b shows x-ray diffraction patterns of the residue obtained at 1075 K after 120 min reaction, and the product simultaneously deposited on the Si substrate at 1050 K by the downstream side of the quartz tube, respectively. The diffraction data (interplanar spacings and peak intensities) determined from the XRD pattern of the residue matched those of hexagonal and tetragonal  $\text{GeO}_2$  phases. No trace of the metallic Ge was observed in the pattern.

The diffraction peaks from the deposit (Fig. 5b) were assigned to the (111), (220), (311), (400), (331), and (422) crystallographic planes with interplanar spacings ( $d$ ) of 0.3220 nm, 0.1984 nm, 0.1695 nm, 0.1408 nm, 0.1293 nm, and 0.1152 nm, respectively. These values are in agreement with the standard data (0.3260 nm, 0.2002 nm, 0.1706 nm, 0.1414 nm, 0.1298 nm, and 0.1155 nm) for Ge with diamond cubic crystal structure (PDF no. 89-3833), indicating that the deposit is metallic Ge. The intensity of the (111) peak is the strongest, as in the standard data, but the intensities of the other peaks are lower. For example, the integrated intensity of the (220) peak is measured to be 7, whereas the standard value is 61.2. This discrepancy is attributed to the preferential growth of Ge (111) grains. It is noted that the peak located at  $2\theta = 69.68^\circ$  ( $d = 0.1348$  nm) belongs to the (400) crystal plane ( $d = 0.1358$  nm) of the Si substrate with an orientation of  $\langle 100 \rangle$ .

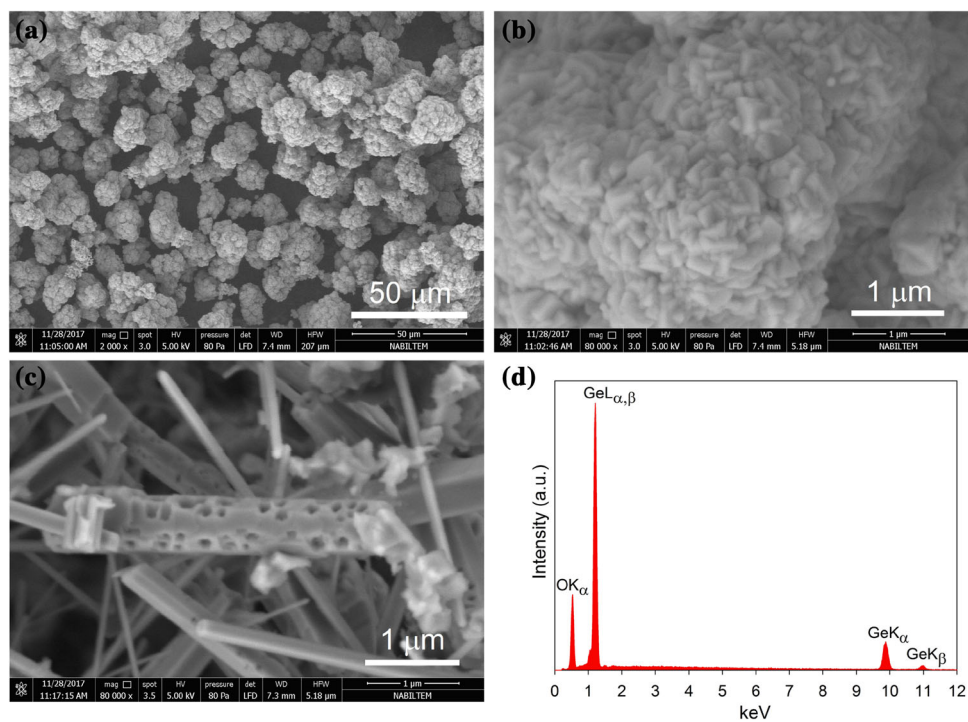


Fig. 3. SEM images of GeO<sub>2</sub> powder used (a) at low magnification, and (b) at high magnification. (c) SEM image of the product remained in the alumina boat after the reaction of GeO<sub>2</sub> powder with CH<sub>4</sub> for 120 min at 1075 K. (d) EDX spectra of the residue.

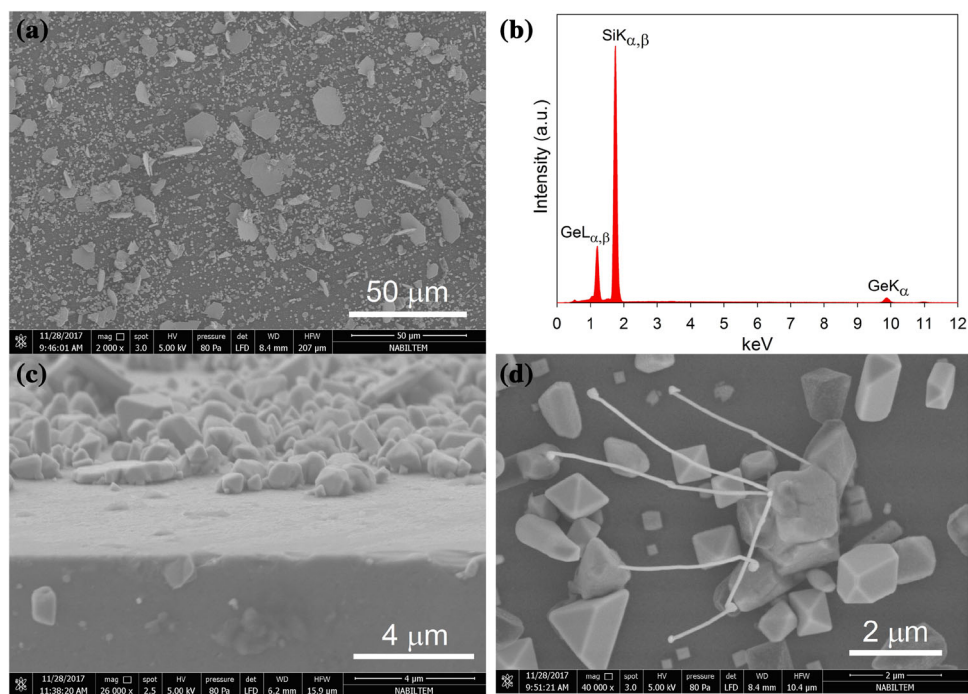


Fig. 4. (a) Surface view of the product deposited on a silicon (100) substrate arbitrarily located at 1050 K in the downstream side of the reaction tube during the reaction of the oxide powder with CH<sub>4</sub> at 1075 K for 120 min. (b) EDX spectrum obtained from image (a). (c) Side view of the product deposited on the Si substrate. (d) Surface view of the deposit.

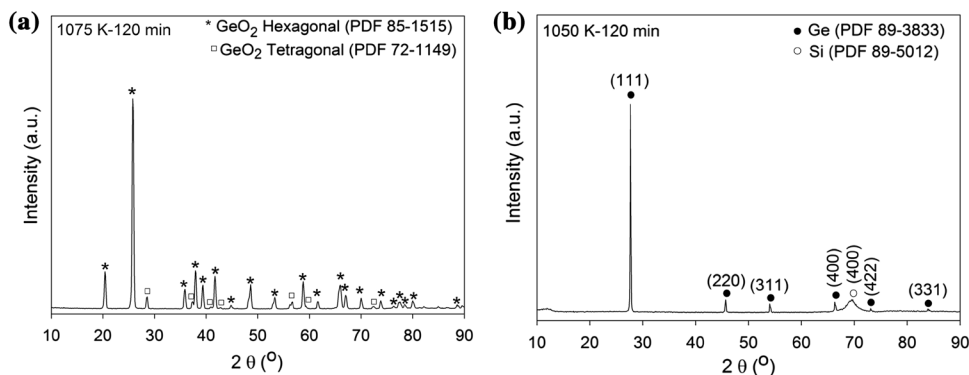
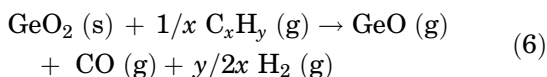


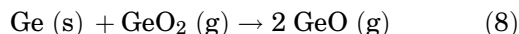
Fig. 5. (a) XRD pattern of the residue in the alumina boat obtained after the reaction of GeO<sub>2</sub> with CH<sub>4</sub> at 1075 K for 120 min. (b) The product simultaneously deposited on the Si substrate at 1050 K by the downstream side of the reaction tube.

### Reaction Pathways to Ge

The reaction pathways leading to the Ge formation from GeO<sub>2</sub> in CH<sub>4</sub> flow may be explained as follows (refer to online supplementary material Fig. S-3). It is postulated that methane cracks into the reducing species of H<sub>2</sub>, C<sub>x</sub>H<sub>y</sub> in the gas phase, prior to the reaction with GeO<sub>2</sub>. These species diffuse into the powder bed and are adsorbed on the GeO<sub>2</sub> particles. The reactions between the oxide particles and the species result in the mass loss. The partial pressure of gaseous GeO species in the Ge-O-C-H system is computed to be relatively high (e.g.,  $\sim 10^{-2}$  atm at 1100 K for  $X_{\text{CH}_4} < 0.4$ ) compared to those of GeH<sub>4</sub> and Ge ( $< 10^{-6}$  atm). It was also reported<sup>2,3</sup> that GeO<sub>2</sub> sublimates via GeO in H<sub>2</sub> atmosphere. Therefore, it is plausible to propose that the mass loss observed in the present study is attributed to the oxide sublimation in the form of GeO. GeO may be produced by the following reactions:



It is also possible that Ge forms on the oxide particle surfaces. The element may then react with GeO<sub>2</sub> to produce volatile GeO species<sup>9</sup> by the following reaction:



This reaction may not be significant in the formation of GeO owing to sluggish solid–solid reaction. The product GeO diffuses into the main gas stream, and is swept away by the gas flow. This diminishes its proportion above the powder bed leading to the high GeO concentration gradient, which, in turn, increases the oxide sublimation rate. In the downstream section of the tube, the reducing conditions appear to be still present. The gaseous GeO is reduced to Ge by the CH<sub>4</sub> decomposition by-

products (e.g., H<sub>2</sub>, CO and C<sub>x</sub>H<sub>y</sub>) via the reactions analogous to Eqs. 5–7. For this, the following reaction may be given as an example:



In the reduction of GeO<sub>2</sub> and GeO, H<sub>2</sub> may be considered as the dominant species as it has low mass and small size (high diffusivity), and the highest concentration in the gas phase amongst the reducing species.

The thermodynamics predicts that free C coexists with Ge. However, C was not detected in the products by XRD and SEM–EDS. It is reported that CH<sub>4</sub> decomposes slightly at temperatures below 1200 K.<sup>10</sup> Hence, no significant C is formed due to sluggish CH<sub>4</sub> decomposition at the temperatures studied (885–1075 K). The white color of the residue at 1075 K may be indicative of the absence of free C. However, small amounts of C may be present as solute and free C in the Ge products because the analytical techniques used are not sensitive. Solubility of C in Ge is reported to be very small ( $< 0.1$  at.%).<sup>11</sup> Zone refinement technique may be used to reduce the contaminant in the product. The technique is also applied to the H<sub>2</sub>-reduced Ge to produce electronic grade Ge.<sup>1</sup> It is proposed that free C can be physically separated from Ge, as they are immiscible when the mixture is heated above the melting of Ge (1210 K). Because liquid Ge does not wet carbon surfaces, graphite-lined tubes have been used for zone refinement of Ge. This indicates that C contamination from graphite is not significant. Even though the quality of the product obtained in the present study may be unsuitable for optical or electronic devices, it can be used as an alloying element in steels and in Argonium™ Sterling Silver.

It should be mentioned that this study might be extended to the recycling of GeO<sub>2</sub>-containing scraps such as ground SiO<sub>2</sub>-GeO<sub>2</sub> glass (optical fiber). SiO<sub>2</sub> is essentially stable in CH<sub>4</sub> flow at the temperatures studied,<sup>10</sup> suggesting that GeO<sub>2</sub> in glass may selectively sublime and be reduced to Ge in a stream of CH<sub>4</sub>.

## CONCLUSION

The reactivity between  $\text{GeO}_2$  and  $\text{CH}_4$  at 885 K and 1025 K is relatively poor owing to the high stability of  $\text{CH}_4$ . The  $\text{CH}_4$  decomposition at 1075 K suffices for the reduction of  $\text{GeO}_2$ . The substantial mass loss observed at this temperature is attributed to the oxide sublimation in the form of  $\text{GeO}$ . Metallic Ge forms from the sublimed oxide transported by the gas flow to the downstream side of the reactor tube. It is proposed that the reduction reactions take place between the oxides and by-products of  $\text{CH}_4$  decomposition. This study demonstrates that Ge can be obtained from  $\text{GeO}_2$  in  $\text{CH}_4$  flow.

## ELECTRONIC SUPPLEMENTARY MATERIAL

The online version of this article (<https://doi.org/10.1007/s11837-018-3039-1>) contains supplement-

tary material, which is available to authorized users.

## REFERENCES

1. R.R. Moskalyk, *Miner. Eng.* 17, 393 (2004).
2. A.P. Hagen, *Inorganic Reactions and Methods: The Formation of Bonds to C, Si, Ge, Sn Pb (Part 1)* (Hoboken: Wiley, 2009).
3. H. Baba, *Bull. Chem. Soc. Jpn.* 29, 789 (1956).
4. S. Cetinkaya and S. Eroglu, *JOM* 69, 993 (2017).
5. M.C. Altay and S. Eroglu, *Metall. Mater. Trans. B* 48B, 2067 (2017).
6. G. Eriksson, *Chem. Scripta* 8, 100 (1975).
7. M.W. Chase, C.A. Davies, J.R. Downey, D.J. Frurip, R.A. McDonald, and A.N. Syverud, *J. Phys. Chem. Ref. Data* 14, 1 (1985).
8. I. Barin, *Thermochemical Data of Pure Substances*, 2nd ed. (Weinheim: VCH Verlagsgesellschaft, 1993).
9. R. Hasegawa, T. Kurosawa, and T. Yagihashi, *Trans. JIM* 13, 39 (1972).
10. S. Cetinkaya and S. Eroglu, *Int. J. Refract. Met. Hard Mater.* 29, 566 (2011).
11. G. Wang, M. Zhang, Y. Zhu, G. Ding, D. Jiang, Q. Guo, S. Liu, X. Xie, P.K. Chu, Z. Di, and X. Wang, *Sci. Rep.* 3, 2465 (2013).